

Oligomerization of the chromatin-structuring protein H-NS

Clare P. Smyth,¹ Thomas Lundbäck,¹ Debora Renzoni,¹ Giuliano Siligardi,² Rebecca Beavil,³ Meredith Layton,⁴ Julie M. Sidebotham,⁵ Jay C. D. Hinton,⁵ Paul C. Driscoll,^{1,4} Christopher F. Higgins^{5,6} and John E. Ladbury^{1*}

¹Department of Biochemistry and Molecular Biology, University College London, Gower Street, London, WC1E 6BT, UK.

²EPSRC National Chiroptical Spectroscopy Centre, Kings College London, Department of Pharmacy, Manresa Road, London, SW3 6LX, UK.

³The Randall Institute, Kings College London, 26–29 Drury Lane, London, WC2B 5RL, UK.

⁴The Ludwig Institute for Cancer Research, 91 Riding House Street, London, W1P 8BT, UK.

⁵Nuffield Department of Clinical Biochemistry, Institute for Molecular Medicine, University of Oxford, John Radcliffe Hospital, Oxford, OX3 9DS, UK.

⁶MRC Clinical Sciences Centre, Imperial College School of Medicine, Hammersmith Hospital, DuCane Road, London, W12 0NN, UK.

Summary

H-NS is a major component of the bacterial nucleoid, involved in condensing and packaging DNA and modulating gene expression. The mechanism by which this is achieved remains unclear. Genetic data show that the biological properties of H-NS are influenced by its oligomerization properties. We have applied a variety of biophysical techniques to study the structural basis of oligomerization of the H-NS protein from *Salmonella typhimurium*. The N-terminal 89 amino acids are responsible for oligomerization. The first 64 residues form a trimer dominated by an α -helix, likely to be in coiled-coil conformation. Extending this polypeptide to 89 amino acids generated higher order, heterodisperse oligomers. Similarly, in the full-length protein no single, defined oligomeric state is adopted. The C-terminal 48 residues do not participate in oligomerization and form a monomeric, DNA-binding domain. These N- and C-terminal domains are joined via a flexible linker which enables them to function independently within

the context of the full-length protein. This novel mode of oligomerization may account for the unusual binding properties of H-NS.

Introduction

The bacterial chromosome is efficiently packaged into a compact structure, the nucleoid (Drlica and Rouviere-Yaniv, 1987; Pettijohn, 1988). However, the expression of a significant proportion of the genome at any one time, and rapid cell doubling times, require a dynamic structure and organization able to respond rapidly to changes in environmental conditions as gene expression is modulated.

A number of DNA-binding proteins have been implicated in the organization of bacterial chromatin (Spassky *et al.*, 1984; Drlica and Rouviere-Yaniv, 1987). The two most abundant of these are HU and H-NS. H-NS is an approximately 15 kDa protein that is present at 10^5 copies cell⁻¹ (Higgins *et al.*, 1990; Ussery *et al.*, 1994; Williams and Rimsky, 1997). H-NS binds DNA in a relatively sequence-independent manner, and although a preference for intrinsically curved sequences has been reported (Bracco *et al.*, 1989; Yamada *et al.*, 1990; Owen-Hughes *et al.*, 1992), this cannot fully explain its mode of action *in vivo* (Jordi *et al.*, 1997). H-NS has also been implicated as a global regulator of gene expression (Higgins *et al.*, 1988; Hulton *et al.*, 1990; Laurent-Winter *et al.*, 1997). Based on this lack of sequence specificity for binding DNA, and the fact that H-NS influences DNA topology *in vivo* and *in vitro* (Higgins *et al.*, 1988; Hulton *et al.*, 1990; Tupper *et al.*, 1994), the mechanism by which H-NS influences transcription is likely to differ from that of more typical sequence-specific transcriptional regulators.

H-NS is an unusual protein because within as few as 136 residues genetic data have indicated that there are at least two distinct functional domains. Genetic data suggest that oligomerization of H-NS is likely to be important for its function (Ueguchi *et al.*, 1996; 1997; Williams *et al.*, 1996). The oligomeric state of H-NS has variously been reported as a dimer, trimer, tetramer or hexamer, depending on experimental conditions and method of analysis (Falconi *et al.*, 1988; Spurio *et al.*, 1997; Ueguchi *et al.*, 1997). It has been established that the N-terminal two-thirds of H-NS (residues 1–91) is sufficient for self-association to occur, whereas the C-terminus is required for DNA binding (Ueguchi *et al.*,

Received 11 October, 1999; revised 7 March, 2000; accepted 11 March, 2000. *For correspondence. E-mail j.ladbury@biochem.ucl.ac.uk; Tel. (+44) 02076 797012; Fax (+44) 020276 797193.

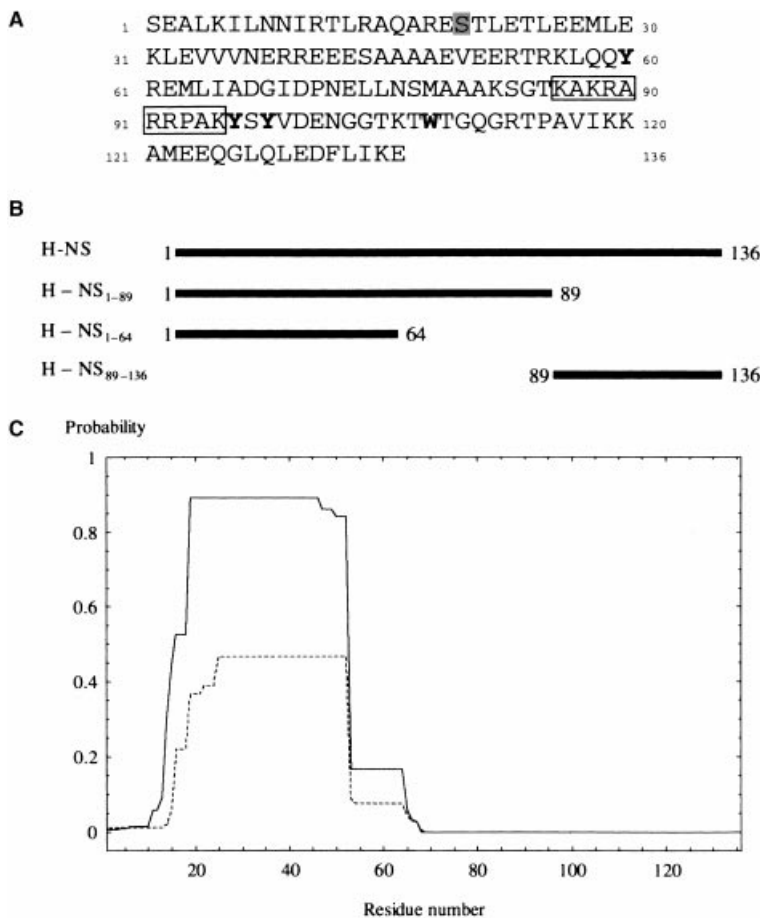


Fig. 1. A. Primary sequence of H-NS from *S. typhimurium* using the one letter codes for the amino acids (Hulton *et al.*, 1990). The protein used in this study had the naturally occurring cysteine at position 20 mutated to a serine residue (grey box). Highlighted in bold are the fluorescent tyrosine and tryptophan residues. A putative DNA-binding region, which is possibly unstructured in the uncomplexed protein (see *Results*) and is abundant in basic residues is boxed.

B. Schematic illustration of full-length H-NS and the three C-terminally and N-terminally truncated forms of H-NS used in this study. All the N-terminal forms had the cysteine to serine mutation at position 20.

C. Prediction of coiled-coil structure in the N-terminal parts of H-NS using the COILS program (version 2.1; 31). The probability for coiled-coil formation is reported as a function of residue number in H-NS, using the scoring matrixes MTK (---) and MTIDK (—). A window of 28 residues was used as recommended for predictions of new coiled-coils. To reduce the possibility of generating false positives, the program's weighting option was employed (i.e. the two hydrophobic positions a and d of the heptad repeat are assigned the same weight as the five hydrophilic positions b, c, e, f and g, see Lupas, 1996).

1996; Williams *et al.*, 1996). However, it has also recently been suggested that mutations in the C-terminus of the protein may also influence its self-associated state (Spurio *et al.*, 1997). Genetic data have also led to the suggestion that H-NS consists of at least three functional domains, responsible for self-association, transcriptional repression and DNA-binding respectively (Ueguchi *et al.*, 1997).

In order to gain a more complete understanding of the mode of action of H-NS, how it compacts bacterial DNA and influences transcription at specific promoters, it is essential to determine in detail its oligomeric state and the residues which contribute to this. We therefore applied a number of complementary biophysical techniques to examine the self-associated state of H-NS from *Salmonella typhimurium* under equilibrium conditions, over a concentration range from the low μM to mM. These data are consistent with a model in which H-NS is composed of two structurally independent domains. These N- and C-terminal domains are joined by a flexible linker. The C-terminal DNA-binding domain plays no role in oligomerization. The N-terminal 64 amino acids of H-NS form stable trimers. Extending the polypeptide to incorporate

residues 65–89 results in the formation of an unusual higher order heterodisperse oligomeric form of the protein. This heterodisperse oligomeric state is maintained in the full-length protein. These unique properties suggest a mechanism by which H-NS is able to condense DNA in the bacterial nucleoid.

Results

We have investigated the domain structure of H-NS directly using biochemical and biophysical methods. Taking a reductionist approach, we investigated selected polypeptide sequences from H-NS of *S. typhimurium* to enable assignment of structural properties to distinct regions within the primary sequence. The polypeptides were chosen based on structural prediction data (see below) and previously reported soluble truncated forms of H-NS (Shindo *et al.*, 1995; Ueguchi *et al.*, 1997). The following three polypeptides were investigated: N-terminal residues 1–64 and 1–89 and C-terminal residues 89–136 (Fig. 1A and B). The properties of these polypeptides were used to obtain an understanding of the oligomerization properties of full-length H-NS. H-NS_{C20S} (H-NS with

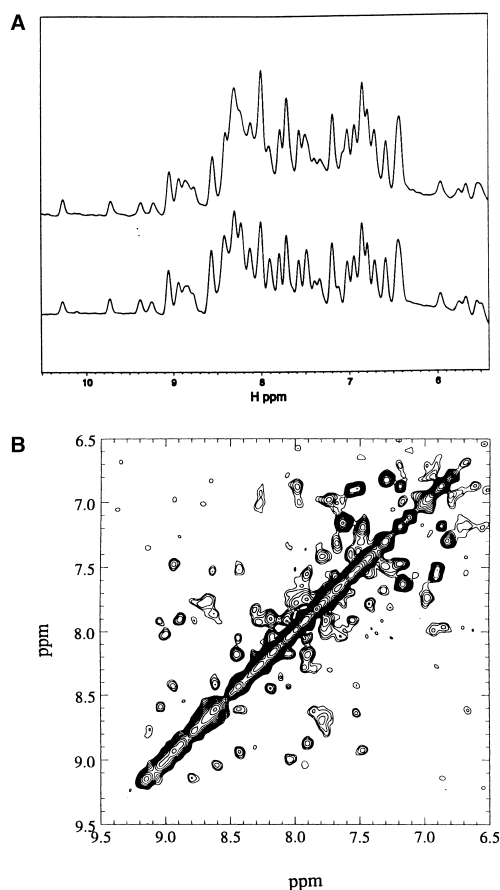


Fig. 2. A. Comparison of the amide region of the 1D ^1H spectra for full-length H-NS (top) and H-NS_{89–136} (bottom) at 20°C. The buffer was 20 mM KPi , 300 mM NaCl and 0.02% sodium azide at pH 7.1 (H-NS) and pH 5.6 (H-NS_{89–136}), respectively, with 10% D_2O added to these buffers. The protein concentrations were 0.6 mM (H-NS) and 0.54 mM (H-NS_{89–136}) respectively. B. The amide region of the 2D ^1H NOESY spectrum of H-NS_{1–64} at 25°C in a buffer containing 20 mM KPi , 300 mM NaCl and 0.02% sodium azide at pH 7.0, with 10% D_2O added to this buffer. The protein concentration was 1.2 mM and the NOESY mixing time was 70 ms. The dispersion of the signals and the NH-NH connectivities provide evidence for a folded protein and of the presence of a α -helical secondary structure.

cysteine at position 20 replaced by serine) was used for all these experiments because it has the same CD spectrum, melting characteristics and similar DNA binding properties as the wild-type protein, but obviates the potential complexities of disulphide bond formation in biophysical experiments. The C20 residue is not highly conserved between bacterial H-NS proteins (Dorman *et al.*, 1999).

NMR spectroscopic analysis of H-NS

Nuclear Magnetic Resonance (NMR) spectra of full-length H-NS_{C20S} showed a limited number of observable peaks, consistent with a significant line broadening effect causing

a large number of peaks to become invisible. This effect usually results from large molecules for which the tumbling times are extended. However, H-NS is only 136 residues and thus, in isolation, should not suffer from this phenomenon. The data suggest therefore, that the protein exists in a self-associated state. Comparison of the NMR spectra for full-length H-NS and the C-terminal polypeptide (residues 89–136) showed that the 1D ^1H NMR spectra were almost identical to each other (Fig. 2A). This is despite the fact that H-NS_{89–136} constitutes only one-third of the full-length protein (Fig. 1B). These initial findings were confirmed by 2D ^1H , ^{15}N -HSQC NMR spectra (data not shown) in which H-NS_{89–136} yielded essentially identical spectra to the full-length protein. The dispersion and overall pattern of chemical shifts observed suggest: (i) that the C-terminal domain has an identical structure in isolation as it does in the intact protein; and (ii) that the first 88 residues of H-NS do not give rise to significant NMR resonances in the intact protein. These results suggest a model in which the C-terminus (residues 89–130) is highly mobile, even within the context of the intact protein, whereas the N-terminal region exists in a self-associated state. Within the context of the intact protein this can only occur if these domains are separated by a highly flexible amino acid linker.

The N-terminus of H-NS (residues 1–64) forms a trimer

Gel-filtration experiments were performed on H-NS_{1–64} over an extensive range of concentrations from 9 μM to 0.62 mM. H-NS_{1–64} adopted a defined oligomeric state, which was invariant in this concentration range (compare with inset in Fig. 3A). Compared with protein molecular weight standards, H-NS_{1–64} had an apparent molecular weight between that of a trimer and a tetramer (i.e. 23.8–31.8 kDa respectively; see inset to Fig. 3C). The fact that the apparent molecular weight was between a trimer and a tetramer could reflect the fact that the oligomeric protein does not adopt a globular fold (see below). To determine more accurately the oligomeric state, analytical ultracentrifugation (AUC) sedimentation equilibrium was used. The data demonstrated that the stable oligomeric state adopted by H-NS_{1–64} is, in fact, a trimer (Fig. 4). Based on experiments performed at three different rotor speeds, using protein concentrations of 0.43 mM (data not shown) and 0.57 mM, an average molecular weight of 22.6 ± 0.6 kDa ($n = 2.84 \pm 0.07$) was calculated using $v = 0.7294 \text{ cm}^3 \text{ g}^{-1}$ and $\rho = 1.0134 \text{ g cm}^{-3}$ (see *Experimental procedures*). The correlation between the size of the 1–64 oligomer at 25°C in gel-filtration studies and at 4°C by AUC shows that the trimer is stable over this temperature range. This observation was corroborated by differential scanning calorimetric data, which showed no

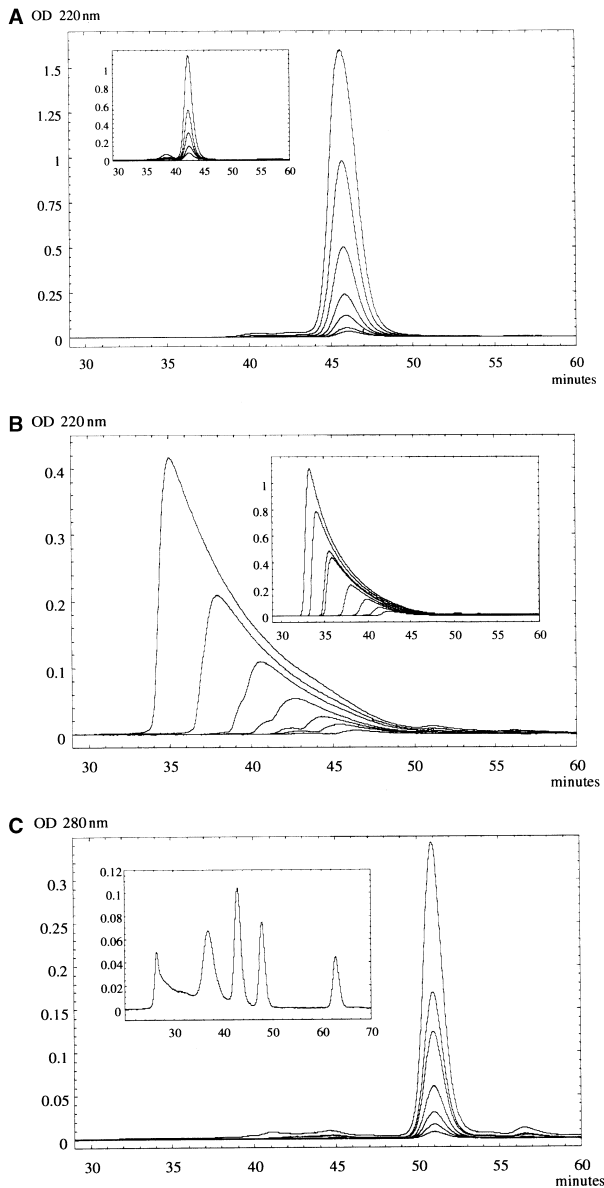


Fig. 3. Gel-filtration assay on full length and truncated forms of H-NS_{C20S}. The figures give the optical density at 220 nm as a function of elution time (minutes). The samples were applied to a Superose 12 column in 20 mM KP_i and 300 mM NaCl at pH 7.0 and 25°C at the indicated concentrations unless otherwise stated. A. H-NS₁₋₆₄ at 9.6, 19.3, 38.5, 77.1, 155, 308 and 617 μ M. The inset gives the traces obtained for a monomeric control protein (ovalbumin) at concentrations ranging from 3 to 49 μ M. B. H-NS₁₋₈₉ at 8.9, 17.9, 35.7, 71.5, 143, 286 and 572 μ M. The inset shows the results on full-length H-NS at 8.9, 17.9, 35.7, 71.4, 143, 162, 260 and 344 μ M. C. H-NS₈₉₋₁₃₆ at 13.4, 26.6, 52.6, 105, 210, 289 and 578 μ M in 1.8 mM KP_i, 10 mM NaP_i, 140 mM NaCl and 2.7 mM KCl at pH 7.4 and 25°C. The optical density was recorded at 280 nm. Given in the inset is the result observed for a molecular weight standard set, with molecular weights of 1.25, 17, 44 and 158 kDa from right to left. There is also an undefined peak corresponding to the void volume and a 660 kDa protein standard (not used in the analysis).

change in excess heat capacity in this temperature range (data not shown), consistent with no change in oligomeric state over the physiological temperature range.

The trimeric region of H-NS is primarily α -helical

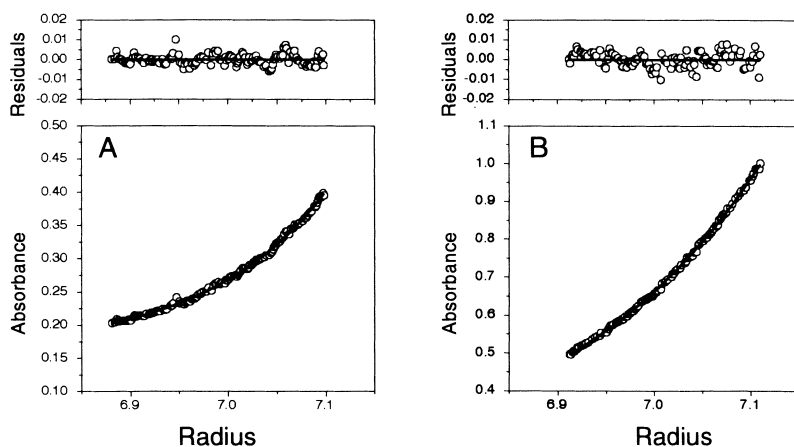
Computer-based structural prediction programs (Lupas, 1996) showed that the N-terminal 64 residues possess a tendency to adopt a coiled-coil motif (Fig. 1C). The presence of a characteristic heptad repeat in these N-terminal amino acids, and sequence similarity to well-known coiled-coil proteins, such as myosin, keratin, and dystrophin led to the suggestion that the self-association of H-NS could be mediated by interactions between α -helices (Ussery *et al.*, 1994). This coiled-coil conformation presumably provides the structural basis for self-association into the trimer.

To test these predictions, circular dichroism (CD) spectrometry was used. The magnitude of the CD in the peptide backbone region between 185 and 260 nm of H-NS₁₋₆₄ was strongly concentration dependent in the range 0.3–30 μ M (in 10 mM KP_i, 10 mM NaCl at pH 7.0). Changes in the CD spectra were pronounced in the two negative maxima at close to 208 and 222 nm and the positive maximum at close to 192 nm (Fig. 5A), demonstrating that the self-association of H-NS₁₋₆₄ is coupled to the formation of a α -helical structure (Table 1). This is consistent with a coiled-coil structure. At concentrations above 30 μ M, no change in CD spectra was observed, indicating that a defined structural state had been attained (Fig. 5A).

Residues 1–64 of H-NS gave measurable NMR spectra (Fig. 2B), in contrast to their behaviour in the context of the intact protein. The limited line broadening and relaxation data were consistent with H-NS₁₋₆₄ forming a defined oligomeric state with a molecular weight significantly less than the large disperse oligomers formed by full-length H-NS (see above). The spectra obtained were also consistent with a significant proportion of a α -helical structure (Fig. 2B).

H-NS₁₋₈₉ adopts higher self-associated states

Compared with H-NS₁₋₆₄, significant NMR spectral line width broadening was observed for H-NS₁₋₈₉. This suggested that residues from 64 to 89 might contribute to the formation of higher order structures. We therefore investigated the oligomerization properties of H-NS₁₋₈₉. Gel-filtration traces obtained for H-NS₁₋₈₉ at a range of concentrations are shown in Fig. 3B. The asymmetric nature of the broad peaks (in marked contrast to H-NS₁₋₆₄) are consistent with H-NS₁₋₈₉ adopting a wide range of different self-associated states with an increased average molecular weight at increased concentrations.



A: H-NS 300mM NaCl 8000rpm $M(1-\nu\rho) = 37176$
 B: H-NS (N-term) 300mM NaCl 15500rpm $M(1-\nu\rho) = 5876$

Fig. 4. Analytical ultracentrifugation sedimentation equilibrium data on H-NS₁₋₆₄ at 0.57 mM at centrifugation speeds of A 8000 and B 15500 r.p.m. The experiments were carried out in 20 mM KP₁ and 300 mM NaCl at pH 7.0 and 4°C. The solid lines represent best-fits with $M(1-\nu\rho)$ values of 37176 and 5876 for these protein solutions. The residuals of the fits are shown in each case, demonstrating that these are randomly distributed around zero.

Distinct oligomeric states could not be resolved. Comparison of peak maxima (Fig. 3B) with globular protein molecular weight standards gave apparent molecular weights ranging from 24 kDa at 8.9 μ M to 198 kDa at 0.57 mM. These numbers correspond to a change in the most abundant oligomeric state of H-NS₁₋₈₉ from somewhat larger than a dimer to something in the order of 20mers within this concentration range. The gel-filtration experiments, despite the potential inaccuracies in determining the molecular weight of the 1-89 polypeptide oligomer, do serve to demonstrate very clearly a difference in behaviour when compared with the 1-64 polypeptide.

We next used AUC to determine the oligomeric state of the 1-89 polypeptide. Again, and in contrast to H-NS₁₋₆₄, AUC data for H-NS₁₋₈₉ could not be accurately modelled for a single species. The average buoyant molecular mass of this polypeptide was found to vary significantly with centrifugation speed, ranging from approximately 68 kDa at 8000 r.p.m. to 32 kDa at 12000 r.p.m. for a protein concentration of 0.58 mM. The increase of $M(1-\nu\rho)$ with decreasing rotor speed demonstrated that H-NS₁₋₈₉ did not reach an equilibrium distribution of oligomeric states at this concentration. As the speed was reduced, the extent to which the larger components could contribute to the average molecular weight of the sample increased, indicating that at the faster speeds the larger complexes travelled to the bottom of the cell and were not detected. It is important to note that the sample did not exhibit time-dependent aggregation, because the observed masses did not depend on the order of data collection at the different speeds. The AUC experiments show that H-NS₁₋₈₉ forms self-associated complexes of considerable size, in agreement with the above gel-filtration data. These data clearly demonstrate dramatically different oligomerization behaviour to trimeric H-NS₁₋₆₄.

The C-terminal domain of H-NS (residues 89-136) is a monomer

Gel-filtration traces for H-NS₈₉₋₁₃₆ at a range of concentrations suggested a molecular weight that is between that predicted for a monomer and a dimer (Fig. 3C). The symmetrical nature of the gel filtration peaks at all concentrations, and the constant position of the peak, confirmed that H-NS₈₉₋₁₃₆ is present in a single, defined state that is concentration independent. AUC sedimentation equilibrium data for H-NS₈₉₋₁₃₆ gave an apparent stoichiometry of 1.3 (data not shown). We interpret these data as showing that the polypeptide is monomeric and attribute the intermediate stoichiometries to possible partial unfolding of this polypeptide, in agreement with the solution structural data for H-NS₉₁₋₁₃₆ from *Escherichia coli* in which some structural disorder was observed (Shindo *et al.*, 1995).

CD spectra for the H-NS₈₉₋₁₃₆ polypeptide were significantly different from those of the N-terminal domain (inset Fig. 3A). The spectra were not dominated by α -helix, in agreement with the previously reported NMR structure for C-terminal H-NS from *E. coli* (Shindo *et al.*, 1995). We can not explain the very small concentration dependence seen in the CD spectra for H-NS₈₉₋₁₃₆ (see inset to Fig. 5B), but note that the magnitude is close to the experimental uncertainty.

The C-terminal (residues 89-136) forms an independent domain within the context of the full-length protein

The observation that only residues 89-136 contributed to the NMR spectra of H-NS_{C20S}, and the location of trypsin-sensitive cleavage sites between residues 82-90 (Cusick and Belfort, 1998), suggest that H-NS₈₉₋₁₃₆ exists as an independent domain within the context of the intact protein. We set out to test this experimentally. Melting

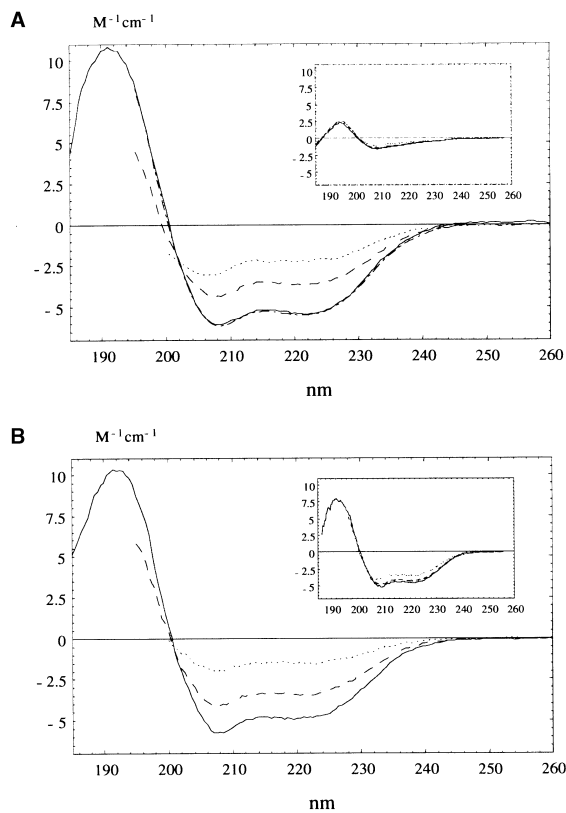


Fig. 5. Circular dichroism studies on full length and truncated forms of H-NS in 10 mM KP_i and 10 mM NaCl at pH 7.0 and 25°C unless otherwise stated. The figures show the delta epsilon $\Delta\epsilon$ as a function of wavelength (λ) in the peptide backbone region (185–260 nm).

A. H-NS_{1–64} at 0.33 (....), 3.3 (– –), 33 (—) and 166 (– · –) μ M showing that the full-length spectrum is dominated by contributions from the N-terminal 64 residues. The inset gives the spectrum of H-NS_{89–136} at 0.32 (....), 3.2 (– –), 32 (—) and 75.5 (– · –) μ M in 5 mM KP_i and 10 mM NaCl at pH 7.0 and 25°C. The C-terminal part of the protein gives a comparatively weak CD spectrum. The small changes in the CD spectrum of H-NS_{89–136} with concentration are negligible in comparison with those observed in full-length H-NS and H-NS_{1–64}.

B. Full-length H-NS at 0.31 (....), 3.1 (– –) and 31 (—) μ M. The inset shows the spectrum of full-length H-NS at 3.1 (....), 31 (– –) and 310 (—) μ M in 10 mM KP_i and 300 mM NaCl at pH 7.0 and 25°C (lower protein concentrations could not be examined due to the strong absorption of buffer components in longer path-length cells).

studies using NMR involve measuring the change of a given proton chemical shift from a particular residue as the protein is heated. The chemical shifts at high field resonances of individual residues in the C-terminal domain can be followed as a function of temperature for H-NS_{89–136} using NMR spectroscopy. The temperature dependence of the chemical shift at 0.12 p.p.m. (20°C) is shown in Fig. 6A. The absence of a clear high temperature end-point prevents a precise determination of the melting temperature (T_m), but an approximate measure can be obtained by fitting for the T_m while floating the high

temperature chemical shift. This results in an apparent T_m of 61°C for H-NS_{89–136} (pH 5.6) using a two-state transition model. Chemical shift data for the full-length protein (as described for H-NS_{89–136} above) shows a transition with a T_m of 58°C (pH 7.0). This is derived from chemical shifts identified as being associated with protons in the C-terminal domains (because the N-terminal suffers from severe line broadening in the full-length NMR spectra). Because the majority of aromatic residues are found in the C-terminus of H-NS, the thermal melting of full-length H-NS (at 31 μ M) was also measured using CD spectroscopy. Analysis of the temperature-induced changes in the aromatic region at 288 nm (Fig. 6B) gave a T_m of 59°C. The T_m values for H-NS_{C20S} were in good agreement with those of the isolated domain, suggesting that the presence of the N-terminal region of the protein has little effect on the stability of the C-terminus. This is consistent with H-NS_{89–136} being a structurally independent domain existing as a monomer (see above) and rules out the possibility of inter-domain interactions. The inability of residues 89–136 to associate within the context of the full-length protein is a requirement for the highly mobile domain required to produce the NMR spectra described above.

The melting temperature derived for the C-terminal domain correlates well with a previously reported value of around 57°C derived from fluorescence spectroscopic studies on *E. coli* H-NS (Tippner and Wagner, 1995). This value is also likely to correspond to the melting of the independent region of residues 89–136 because Trp 108 is the major fluorophore in the protein.

Full-length H-NS_{C20S} adopts higher self-associated states

The gel-filtration peaks for H-NS_{C20S} were broad and clearly asymmetric at all concentrations (inset Fig. 3B), as seen for H-NS_{1–89}. These results substantiate the

Table 1. Deconvolution of the circular dichroism data.

Protein/Polypeptide	Concentration (μ M)	α -Helix (%)
H-NS _{C20S}	310	45.3 ^a
	31	47 ^b (44.3 ^a)
	3.1	30.4 ^b (34.4 ^a)
	0.31	14.8 ^b
	166	55
H-NS _{1–64} ^b	33	53.2
	3.3	34.9
	0.33	19.4
H-NS _{89–136} ^c	75.5	10.7
	32	10.5
	3.2	9.6
	0.32	7.8

a. In 10 mM KP_i and 300 mM NaCl at pH 7.0 and 25°C.

b. In 10 mM KP_i and 10 mM NaCl at pH 7.0 and 25°C.

c. In 5 mM KP_i and 10 mM NaCl at pH 7.0 and 25°C.

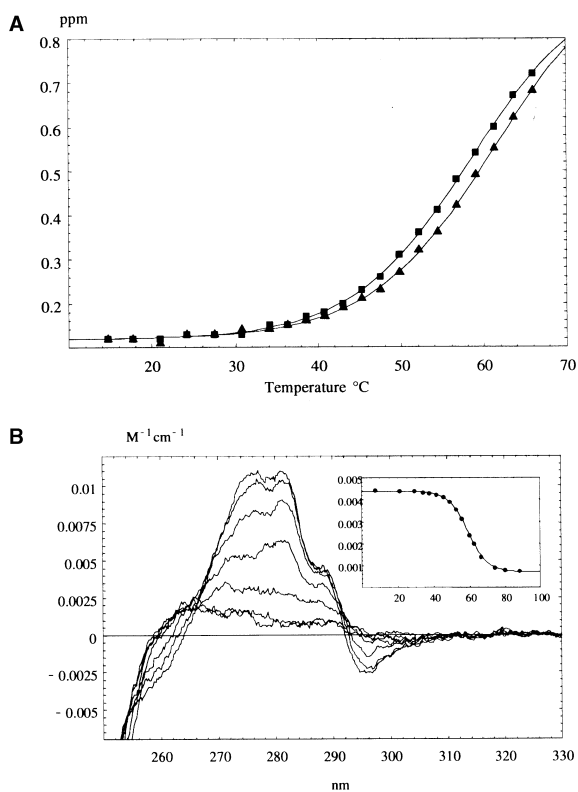


Fig. 6. A. NMR melting experiments of H-NS₈₉₋₁₃₆ and full-length H-NS. The chemical shift at 0.12 p.p.m. (20 °C) was followed as a function of temperature (15–68 °C). The buffer was 20 mM KP_i, 300 mM NaCl and 0.02% sodium azide at pH 7.0 (H-NS) or pH 5.6 (H-NS₈₉₋₁₃₆), respectively, with 10% D₂O and 0.00125% TSP added to these buffers. The protein concentrations were 0.22 mM (H-NS) and 0.54 mM (H-NS₈₉₋₁₃₆) respectively. The change in chemical shift with temperature was fitted to a sigmoidal model, as demonstrated by the solid lines, to obtain an apparent melting point of 58 °C for full-length H-NS (■) and 61 °C for H-NS₈₉₋₁₃₆ (▲) respectively.

B. Aromatic region of the full-length H-NS (31 μM) spectrum at 33.8, 41.3, 48.9, 55.4, 62.5, 74.3 and 88.2 °C. The inset gives the delta epsilon (Δε) at 288 nm as a function of temperature and the solid line represents the non-linear least-square fit to the data with a melting temperature of 59 °C as described in the text.

hypothesis that H-NS_{C20S} self-associates to form large complexes as the concentration is increased, and that no single defined state is reached within the concentration range tested. In this case, a comparison with molecular weight standards gave apparent molecular weights of 51 kDa at 8.9 μM and 281 kDa at 0.34 mM, for these peak maxima. These numbers correspond to a change in the oligomeric state from somewhat larger than a trimer to approximately 20-mers within this concentration range, similar to the data for H-NS₁₋₈₉. The peaks were smooth and distinct oligomeric states could not be resolved even when other columns were used (inset to Fig. 3B).

The behaviour of full-length protein, as observed by AUC, resembled that of H-NS₁₋₈₉ (data not shown). The buoyant molecular mass of H-NS_{C20S} ranged from 37 kDa

at 8000 r.p.m. to 26 kDa at 12000 r.p.m. for a protein concentration of 52 μM. These are lower molecular masses than previously observed for the 1–89 polypeptide, but this can be explained by the significant difference in concentration and protein size (more of the larger H-NS_{C20S} will travel to the bottom of the cell and not contribute to the analysis). Additional AUC sedimentation velocity experiments were carried out on H-NS_{C20S} (data not shown) and a large set of interacting and non-interacting models were used in an attempt to fit the data (including monomer–dimer, monomer–tetramer–octamer, monomer–trimer–hexamer–nonamer). None of these models led to an improved fit of the data and, furthermore, the derivatives of the velocity data curves suggest a multicomponent system. The presence of a range of oligomeric states agrees with the above gel-filtration data, in which the width of the asymmetric peak for any given concentration spans approximately a 10-fold difference in molecular weight.

The behaviour observed on gel filtration could, potentially, be explained if H-NS_{C20S} dissociates from a defined oligomeric state while travelling through the column. This has previously been invoked to explain the behaviour of mutants of the coiled–coil leucine zipper protein GCN4 (Zeng *et al.*, 1997). However, in the light of the above AUC data, we favour the explanation that the protein exists in a range of different oligomeric states.

CD spectra for the full-length H-NS protein were very similar to those obtained for residues 1–64 (Fig. 3B). Again, the CD signal was strongly concentration dependent and accompanied by the formation of an α-helical secondary structure at lower concentrations (Table 1). It was not possible to assess whether the α-helix content reached a maximum at high concentration (as seen in the case of H-NS₁₋₆₄) owing to insolubility of H-NS_{C20S} at 10 mM NaCl. The protein appears to aggregate/precipitate in low saline conditions. Under higher salt conditions (300 mM NaCl), H-NS_{C20S} is soluble and CD spectra at high concentration could be obtained. The CD spectra resembled those observed in low salt conditions. At high protein concentrations (up to 310 μM) the α-helical content of the sample did not increase significantly (Table 1 and inset Fig. 5B), demonstrating that the oligomeric state which is accompanied by structure formation has become saturated. This does not necessarily mean that maximum oligomeric state of H-NS_{C20S} has been achieved, because another mechanism for this self-association, which is not accompanied by additional structure formation, could prevail. Indeed, this appears to be the case because, although the formation of an α-helix has a limit at concentrations in the region above 30 μM, gel filtration as well as AUC experiments show that the formation of higher oligomeric states continues at concentrations above this. These findings are in contrast

to the situation for H-NS_{1–64} (Fig. 3A), which self-associates with the concomitant formation of a α -helix, but once the trimeric form has been reached then no further self-association is observed.

Discussion

Genetic data have demonstrated that H-NS consists of at least two domains and can exist in oligomeric forms that contribute to its biological activity. Biochemical studies of the oligomeric state have, however, led to conflicting conclusions. We have therefore attempted to characterize this behaviour directly using biochemical and biophysical approaches. The data reported here demonstrate that H-NS does not exist in a single, defined, oligomeric state and highlight the complex and unusual nature of H-NS oligomerization. The protein consists of two distinct domains separated by a highly flexible linker. The C-terminal DNA-binding domain (amino acids 89–136) does not contribute to oligomerization and, in the context of the intact oligomeric protein, is freely mobile. Oligomerization is due to the N-terminal domain (residues 1–89). Amino acids 1–64 form a discrete trimer, probably a coiled-coil. The addition of 25 amino acids (residues 1–89) results in the formation of larger, heterodisperse oligomers (up to at least 20 mers) in a concentration-dependent fashion. Full-length H-NS also adopts a concentration-dependent heterodisperse oligomeric state of up to 20 mers.

Trimer formation is biologically relevant because the same residues of H-NS expressed *in vivo* produce a dominant-negative effect when expressed in *hns+* bacteria (Ueguchi *et al.*, 1997). Trimerization probably involves a coiled-coil configuration and we have demonstrated the formation of an increased α -helical structure upon oligomerization. Trimer formation increases with concentration up to about 30 μ M. Trimer formation is also temperature independent, at least within the physiological range. Trimer formation is likely to form a building block for higher order oligomerization.

Increasing the polypeptide length to include residues 65–89 resulted in further self-association, giving rise to heterodisperse, higher order oligomeric states. The size of the oligomers increased with concentration. This oligomerization was also seen in the full-length protein: it appears that residues 65–89 form the platform for this oligomerization.

Remarkably, like residues 1–89, full length also H-NS forms heterodisperse, higher order oligomers in a concentration-dependent fashion. At concentrations below 30 μ M, there is concentration-dependent formation of α -helix, consistent with the building block being the coiled-coil trimers seen for residues 1–64. At higher concentrations, further self-association continued in a

manner similar to that observed for amino acids 1–89. This two-step self-association, the formation of trimers and then association into larger heterodisperse oligomers whose size increases with concentration is a unique property of H-NS and unusual for such a comparatively small protein. The finding that H-NS does not adopt a discrete oligomeric state accounts for published data, which appear, at first sight, inconsistent in reporting oligomeric forms of H-NS from dimer to hexamer (Falconi *et al.*, 1988; Spurio *et al.*, 1997; Ueguchi *et al.*, 1997).

The C-terminal domain of H-NS, in both the free form and covalently associated within the context of the intact protein, was shown by NMR spectroscopy to be structurally independent and isolated by a flexible linker, allowing it a high degree of mobility such that it can rotate freely. The reported structure of the C-terminal of H-NS from *E. coli* (Shindo *et al.*, 1995) shows that the globular fold begins at about residue 95, so the flexible linker is probably included in the H-NS_{89–136} polypeptide. The role of this flexible linker is yet to be resolved; however, it is presumably required for the C-terminal domain to adopt the necessary orientations within a large oligomeric structure in order to interact with DNA.

The high concentration of H-NS in bacterial cells means that the prevalence of high order oligomers will provide a scaffold around which DNA can interact and facilitate its compaction. As the isolated C-terminal domain shows low affinity for DNA (Shindo *et al.*, 1995), it is likely that the cooperative effect of binding of the oligomeric protein leads to enhanced affinity within the context of the full-length protein. The availability of a C-terminal DNA binding domain on a flexible linker avoids steric constraint on the binding of DNA and its subsequent packaging.

Experimental procedures

Bacterial strains and plasmids

E. coli strain DH5 α was used for all gene cloning experiments. Plasmid pJSH6, which encodes the C20S mutant of the full-length H-NS, was constructed as described below. Chromosomal DNA from *S. typhimurium* was purified as described elsewhere (Maniatis *et al.*, 1982). The primers 5'-CAAAGTGGAGACT-CATATGAGCGAAGCACTTAAAATTC-3' and 5'-CACGGATCCGGTT-CCTGGGTATTAAGAAG-TAAC-3' were used to amplify, by PCR, the H-NS structural gene (Hulton *et al.*, 1990), and to introduce *Bam*HI and *Nde*I restriction sites at the 5' and 3' ends respectively. The PCR product was cloned into the *Sma*I site of pT7-3 (Tabor and Richardson, 1985) to generate pJSH1. The *hns* gene was excised from pJSH1 on an *Eco*RI-*Hind*III fragment and subsequently cloned into pALTER for site-directed mutagenesis (Altered Sites 2 system from Promega). The C20S mutation was introduced into the *hns* gene, using the primer 5'-GCGCAGGCAAGAGAAAGCACTCTGGAAACGC-3'. The C20S *hns* gene was completely sequenced to ensure no

other mutations had been introduced. The gene was excised from pALTER with *Bam*HI and *Nde*I and ligated into *Bam*HI–*Nde*I-digested pET14b and named pJSH6 (Studier and Moffat, 1986; Rosenberg *et al.*, 1987). This also introduced an N-terminal 6 × His-tag followed by a thrombin cleavage site.

Plasmids pCPS1 and pCPS2, which overexpress H-NS_{1–64} and H-NS_{1–89} respectively, were constructed. Truncated *hns* genes, coding for residues 1–64 and 1–89, were amplified with pJSH6 as the template, using primers 5′-CAAAGTGGAGACTCATATGAGCGAAGCACTTAAAATT-C-3′ and 5′-CACGGATCCCTATTATAACATTTCACGATAC-TGTTGCAGTTT-3′ or 5′-CACGGATCCCTATTAGCGTTTACGCTTTGGTACCGGATTTAGC-3′ respectively. Restriction sites *Nde*I and *Bam*HI were introduced at the 5′ and the 3′ ends respectively. The PCR products were digested with *Nde*I and *Bam*HI and ligated into pET14(b), introducing an N-terminal 6 × His tag and thrombin cleavage site as described above. DNA sequencing was used to verify the identity of the truncated *hns* genes.

Protein expression, purification and biological activity

E. coli BL21 (λDE3 *plys*S) cells were transformed, separately with plasmids pJSH6, pCPS1 and pCPS2 to express full-length H-NS_{C20S}, H-NS_{1–64} or H-NS_{1–89} respectively. Next, 500 ml flasks containing 150 ml of Luria–Bertani (LB) media, chloramphenicol (34 µg ml⁻¹) and carbenicillin (200 µg ml⁻¹) were inoculated with cells from a freshly transformed colony. Then 10 ml of the overnight cultures were used to inoculate 2 l flasks containing fresh media and antibiotics (500 ml) and grown in a shaking incubator at 200 r.p.m. and 37°C until an OD₆₀₀ of 0.5 was reached. The T7 promoter was then induced by the addition of isopropyl-β-D-thiogalactopyranoside (IPTG; Melford Laboratories) to a final concentration of 0.5 mM and incubated at 200 r.p.m. and 30°C for 3 h. The cells were centrifuged at 5000 r.p.m. in a SORVALL GS3 rotor and the resulting cell pellet was stored at –70°C.

Cell lysis was by sonication in 20 mM Tris, 500 mM NaCl, 5% glycerol, 1% Triton X-100 and 0.5 mM 4-(2-aminoethyl) benzene sulphonyl fluoride hydrochloride (AEBSF; Melford Laboratories) at pH 8.0. The lysate was centrifuged to remove insoluble cell debris. The supernatant was heated to 60°C for 15 min, recentrifuged to remove any denatured protein and applied to a TALON™ metal affinity column equilibrated with 20 mM Tris, 500 mM NaCl and 5% glycerol at pH 8.0. His-tagged H-NS protein was eluted in 20 mM Tris, 500 mM NaCl, 0.5 M imidazole and 5% glycerol at pH 8.0. The protein was precipitated with 70% ammonium sulphate and subsequently resuspended in 20 mM Tris, 150 mM NaCl, 2.5 mM CaCl₂ and 5% glycerol at pH 8.0. Thrombin (Bovine Thrombin, Calbiochem) was added to remove the His-tag, and the protein diluted four times with distilled water and then applied to a Pharmacia MonoS column equilibrated in 10 mM KP_i, 1 mM Na-EDTA at pH 7.5. H-NS was then eluted in 10 mM KP_i, 600 mM NaCl and 1 mM Na-EDTA at pH 7.5. Thrombin cleavage of the His-tag resulted in a protein product with four additional amino acids, GSHM, at the N-terminus of each H-NS-derived protein.

For the purification of H-NS_{1–64} and H-NS_{1–89} polypep-

tides, the heating step after the initial cell lysis and centrifugation steps was not performed. Furthermore, subsequent to thrombin cleavage, the polypeptides were reapplied to the TALON™ metal affinity column and collected as flow through, thus removing the His-tag, which remains bound to the column.

The N-terminally truncated H-NS_{89–136} protein was purified as follows. The supernatant containing full-length His-tagged H-NS_{C20S} protein was applied to the TALON™ metal affinity column equilibrated in 20 mM Tris, 150 mM NaCl and 2.5 mM CaCl₂ at pH 8.0. Trypsin was added to the column, resulting in cleavage of the full-length protein (Cusick *et al.*, 1998). The H-NS_{89–136} polypeptide was eluted with the above buffer. The protein was purified further using the MonoS column as described above.

Full-length H-NS_{C20S}, H-NS_{1–64}, H-NS_{1–89} and H-NS_{89–136} protein samples were concentrated according to the requirements of a given experiment (see below), using either an Amicon stirred cell or centriprep (Amicon) concentrators, and dialysed into the required buffer, depending upon the experiment to be performed. The polypeptides were stored under the experimental buffer at 4°C prior to use.

The size and homogeneity (> 95% in all cases) of the purified proteins was confirmed by denaturing SDS–PAGE and staining with Coomassie brilliant blue R-250. The mass of each of the proteins was confirmed using mass spectrometry. The following results were obtained with the expected molecular weight given within brackets. H-NS_{C20S}, 15806 g mol⁻¹ (15805); H-NS_{1–64}, 7959 g mol⁻¹ (7958); H-NS_{1–89}, 10516 g mol⁻¹ (10512); and H-NS_{89–136}, 5311/5467 g mol⁻¹ (5314/5470). The difference in molecular weight between the two species in the H-NS_{89–136} sample is equivalent to that of an arginine residue, indicating that the trypsin cleavage yields two different products (Cusick *et al.*, 1998). All the experimental results are identical to the expected masses within experimental uncertainty.

The biological activity of the C20S full-length protein was compared with that of wild-type H-NS from *S. typhimurium* (Hulton *et al.*, 1990), using *in vitro* DNA mobility shift assays. Plasmid pAF3 (Jordi *et al.*, 1997) was purified and digested with the restriction enzyme *Hae*III. The DNA restriction fragments were incubated with wild-type H-NS or H-NS_{C20S} (in an overall amount ranging from 0.1 to 6.0 µg), in 10 µl reaction mixtures containing 10 mM Tris, 0.2 mM Na-EDTA, 15 mM KCl, 2 mM spermidine and 15% glycerol at pH 7.5. After 10 min at room temperature, protein–DNA complexes were resolved on 3% agarose gels, using TBE (89 mM Tris-Borate, 89 mM Boric acid and 10 mM Na-EDTA at pH 8.0) as the running buffer. The DNA fragments were stained with ethidium bromide and visualized using a UV lamp. H-NS_{C20S} caused a shift in the mobility of DNA, which was comparable to that of wild-type H-NS (data not shown).

Circular dichroism spectroscopy

Proteins were extensively dialysed against a buffer containing 10 mM potassium phosphate (KP_i) and 10 mM NaCl at pH 7.0 at 4°C unless otherwise stated. H-NS_{89–136} and the full-length H-NS_{C20S} that were to be used for the low temperature study were, instead, dialysed against a buffer

containing 15 mM KP_i and 30 mM NaCl at pH 7.0 and then diluted three times using water and ethanediol respectively. CD spectra were recorded on Jasco 600 or 700 spectropolarimeters with JOVAN attachments for low temperature measurements. Spectra for the peptide backbone region (185–320 nm) were recorded using different path-length cells, ranging from 0.01 to 2 cm, depending on the protein concentration. Spectra for the aromatic region (240–340 nm) were recorded in a 5 cm path-length cell. All spectra were averaged over two or four scans, using a resolution of 0.2 nm and a scan rate of 10 nm per minute. All the samples were allowed to reach thermal equilibrium in the cell, the temperature of which was controlled using a Hewlett Packard peltier system. The estimation of secondary structure content was performed using a principle component regression method (PLSIQPRD of GRAMS/3.2 suite program) with a calibration data set of 16 proteins obtained elsewhere (Hennessey and Johnson, 1981).

Nuclear magnetic resonance spectroscopy

The 1H 1D and 2D Nuclear Overhauser Effect Spectroscopy (NOESY) spectra (Macura *et al.*, 1981) were recorded on a Varian UNITYplus 500 MHz spectrometer. The NMRPIPE (Delaglio *et al.*, 1995) and AZARA 2.0 (Boucher, 1996) software was used to process and analyse the data. Next, 3-(trimethylsilyl)-propionate (TSP) was added to the samples used for the NMR melting studies as an internal standard for the referencing of the proton chemical shifts.

Gel filtration

A range of concentrations of H-NS_{C20S}, H-NS_{1–64}, H-NS_{1–89}, H-NS_{89–136} or a control protein (ovalbumin) were applied to a BIOCAD/INTEGRAL system equipped with a Pharmacia Superose 12 column. All proteins were dialysed against 10 mM KP_i and 300 mM NaCl at pH 7.0 prior to loading the column. The column was equilibrated with either the dialysis buffer or phosphate-buffered saline (PBS) (1.8 mM KP_i , 10 mM NaP_i , 140 mM NaCl and 2.7 mM KCl at pH 7.4) as indicated in the text. A calibration of the expected flow rates was obtained by running molecular weight standards (Bio-Rad Gel Filtration Standard) in 10 mM KP_i and 300 mM NaCl at pH 7.0. These covered the range of molecular weights from 1350 to 670 kDa.

Analytical ultracentrifugation

Analytical ultracentrifugation experiments were performed using a Beckman XL-A analytical ultracentrifuge. Data were acquired as an average of 25 absorbance measurements at a wavelength of 280 nm and a radial spacing of 0.001 cm. H-NS protein was prepared in 20 mM KP_i , 300 mM NaCl and 0.05% sodium azide at pH 7.0. All sedimentation equilibrium experiments were run using double sector charcoal-filled centrepieces and column lengths of approximately 4 mm. Solvent densities were calculated from standard tables (Handbook of Chemistry and Physics, 1968, CRC Press, Oxford). Sedimentation equilibrium experiments were conducted at various rotor speeds, ranging from 8000 to

17000 r.p.m., and temperatures of 4.0, 15.0 and 20°C. The time required for the attainment of equilibrium was established by running at a given rotor speed until successive scans, taken 12 h apart, were invariant. Data were then analysed to obtain the buoyant molecular mass, $M(1 - \nu\rho)$, using the Optima XL-A data analysis software (version 2.0, Beckman) running under Microcal Origin 2.8, by fitting data from each scan to:

$$A_r = \exp(\ln(A_o) + HM(1 - \nu\rho)(r^2 - r_o^2)) + E \quad (1)$$

where A_o is the absorbance at a reference point r_o , A_r is the absorbance at a given radial position r , H represents $\omega^2/2RT$, with ω being the angular speed in rad s^{-1} , R , the gas constant and T the absolute temperature, and E is a small baseline correction term. Residuals were calculated by subtracting the best fit eq. 1 from the experimental data. A modified version of the equation, including terms for self-association or multicomponent systems, was also used (BECKMAN ANALYSIS software version 2.0).

Acknowledgements

We would like to thank D. Ussery for his contribution to initiating this study. J.E.L. is a Wellcome Trust Senior Research Fellow. T.L. was supported by the Swedish Foundation for International Cooperation in Research and Higher Education and the Swedish National Sciences Council. This work was supported by a Wellcome Trust Programme Grant (Ref. 045490) to C.F.H. and J.C.D.H. and by the ICRF.

References

- Boucher, W. (1996) AZARA v2.0. Cambridge, UK: Department of Biochemistry, University of Cambridge.
- Bracco, L., Kotlarz, D., Kolb, A., Diekmann, S., and Buc, H. (1989) Synthetic curved DNA-sequences can act as transcriptional activators in *Escherichia coli*. *EMBO J* **8**: 4289–4296.
- Cusick, M.E., and Belfort, M. (1998) Domain structure and RNA annealing activity of the *Escherichia coli* regulatory protein StpA. *Mol Microbiol* **28**: 847–857.
- Delaglio, F., Grzesisek, S., Vuister, G.W., Zhu, G., Pfeifer, J., and Bax, A. (1995) NMR-Pipe – A multidimensional spectral processing system based on UNIX pipes. *J Biomol NMR* **6**: 277–293.
- Dorman, C.J., Hinton, J.C.D., and Free, A. (1999) Domain organization and oligomerization among H-NS-like nucleoid-associated proteins in bacteria. *Trends Microbiol* **7**: 124–128.
- Drlica, K., and Rouviere-Yaniv, J. (1987) Histone-like proteins of bacteria. *Microb Rev* **51**: 301–319.
- Falconi, M., Gualtieri, M.T., LaTeana, A., Losso, M.A., and Pon, C.L. (1988) Proteins from the prokaryotic nucleoid – Primary and quaternary structure of the 15 kDa *Escherichia coli* DNA-binding protein, H-NS. *Mol Microbiol* **2**: 323–329.
- Hennessey, J., and Johnson, W.C. (1981) Information content in the circular dichroism of proteins. *Biochemistry* **20**: 1085–1094.
- Higgins, C.F., Dorman, C.J., Stirling, D.A., Waddell, L., Booth, I.R., May, G., *et al.* (1988) A physiological role for DNA supercoiling in the osmotic regulation of gene expression in *S. typhimurium* and *E. coli*. *Cell* **52**: 569–584.
- Higgins, C.F., Hinton, J.C.D., Hulton, C.S.J., Owen-Hughes, T., Pavitt, G.D., and Seirafi, A. (1990) Protein H1: a role for

- chromatin structure in the regulation of bacterial gene expression and virulence? *Mol Microbiol* **4**: 2007–2012.
- Hulton, C.S.J., Seirafi, A., Hinton, J.C.D., Sidebotham, J.M., Waddell, L., Pavitt, G.D., *et al.* (1990) Histone-like protein H1 (H-NS), DNA supercoiling and gene expression in bacteria. *Cell* **63**: 631–642.
- Jordi, B.J.A.M., Fielder, A.E., Burns, C.M., Hinton, J.C.D., Dover, N., Ussery, D.W., *et al.* (1997) DNA binding is not sufficient for H-NS mediated repression of *proU* expression. *J Biol Chem* **272**: 12083–12090.
- Laurent-Winter, C., Ngo, S., Danchin, A., and Bertin, P. (1997) Role of *Escherichia coli* histone-like nucleoid structuring protein in bacterial metabolism and stress response. Identification of targets by two-dimensional electrophoresis. *Eur J Biochem* **244**: 767–773.
- Lupas, A. (1996) Coiled-coils: New structures and new functions. *Trends Biochem Sci* **21**: 375–382.
- Macura, S., Huang, Y., Suter, D., and Ernst, R.R. (1981) Two-dimensional chemical exchange and cross-relaxation spectroscopy of coupled nuclear spins. *J Magn Reson* **43**: 259–281.
- Maniatis, T., Fritsch, E.F., and Sambrook, J. (1982) *Molecular Cloning: a Laboratory Manual*. Cold Spring Harbor, NY: Cold Spring Harbor Laboratory Press.
- Owen-Hughes, T.A., Pavitt, G.D., Santos, D.S., Sidebotham, J.M., Hulton, C.S.J., Hinton, J.C.D., *et al.* (1992) The chromatin-associated protein H-NS interacts with curved DNA to influence DNA topology and gene expression. *Cell* **71**: 255–265.
- Pettijohn, D.E. (1988) Histone-like proteins and bacterial chromosome structure. *J Biol Chem* **263**: 12793–12796.
- Rosenberg, H.A., Lade, B.N., Chui, D.S., Lin, S.W., Dunn, J.J., and Studier, F.W. (1987) Vectors for selective expression of cloned DNAs by T7 RNA polymerase. *Gene* **56**: 125–135.
- Shindo, H., Iwaki, T., Ieda, R., Kurumizaka, H., Ueguchi, C., Mizuno, T., *et al.* (1995) Solution structure of the DNA-binding domain of a nucleoid-associated protein, H-NS, from *Escherichia coli*. *FEBS Microbiol Lett* **360**: 125–131.
- Spurio, R., Falconi, M., Brandi, A., Pon, C.L., and Gualerzi, C.O. (1997) The oligomeric structure of nucleoid protein H-NS is necessary for recognition of intrinsically curved DNA and for DNA bending. *EMBO J* **16**: 1795–1805.
- Studier, F.W., and Moffat, B.A. (1986) Use of bacteriophage T7 RNA polymerase to direct selective high level expression of cloned genes. *J Mol Biol* **189**: 113–130.
- Tabor, S., and Richardson, C.C. (1985) A Bacteriophage T7 RNA polymerase promoter system for controlled exclusive expression of specific genes. *Proc Natl Acad Sci USA* **82**: 1074–1078.
- Tippner, D., and Wagner, R. (1995) Fluorescence analysis of the *Escherichia coli* transcription regulator, H-NS reveals two distinguishable complexes dependent on binding to specific or nonspecific DNA sites. *J Biol Chem* **38**: 22243–22247.
- Tupper, A.E., Owen-Hughes, T.A., Ussery, D.W., Santos, D.S., Ferguson, D.J.P., Sidebotham, J.M., *et al.* (1994) The chromatin-associated protein H-NS alters DNA topology in vitro. *EMBO J* **13**: 258–268.
- Ueguchi, C., Suzuki, T., Yoshida, T., Tanaka, K., and Mizuno, T. (1996) Systematic mutational analysis revealing the functional domain organization of *Escherichia coli* nucleoid protein H-NS. *J Mol Biol* **263**: 149–162.
- Ueguchi, C., Seto, C., Suzuki, T., and Mizuno, T. (1997) Clarification of the dimerization domain and its functional significance for the *Escherichia coli* nucleoid protein H-NS. *J Mol Biol* **274**: 145–151.
- Ussery, D.W., Hinton, J.C.D., Jordi, B.J.A.M., Granum, P.E., Seirafi, A., Stephen, R.J., *et al.* (1994) The chromatin-associated protein H-NS. *Biochimie* **76**: 968–980.
- Williams, R.M., and Rimsky, S. (1997) Molecular aspects of the *E. coli* nucleoid protein H-NS: a central controller of gene regulatory networks. *FEMS Microbiol Lett* **156**: 175–185.
- Williams, R.M., Rimsky, S., and Buc, H. (1996) Probing the structure, function, and interactions of the *Escherichia coli* H-NS and StpA proteins by using dominant negative derivatives. *J Bacteriol* **178**: 4335–4343.
- Yamada, H., Muramatsu, S., and Mizuno, T. (1990) An *Escherichia coli* protein that preferentially binds to sharply curved DNA. *J Biochem (Tokyo)* **108**: 420–425.
- Zeng, X., Herdon, A.M., and Hu, J.C. (1997) Buried asparagines determine the dimerization specificities of leucine zipper mutants. *Proc Natl Acad Sci USA* **94**: 3673–3678.